

Improvement of an MPD Thruster Performance with a Laval-type Magnetic Nozzle

IEPC-2005-83

Presented at the 29th International Electric Propulsion Conference, Princeton University,
October 31 – November 4, 2005

M.Inutake ^{*}, A.Ando [†], K.Hattori [‡], H.Tobari [§], K.Harata ^{**}, and T.Komagome ^{††}
Department of Electrical Engineering, Graduate School of Engineering, Tohoku University
6-6-05, Aoba-yama, Sendai, 980-8579, Japan

Abstract: A Laval-type external magnetic nozzle is applied to an MPD thruster in order to improve its performance and the exhausted plasma flow is investigated spectroscopically. By installing a magnetic Laval nozzle near the muzzle of an MPD thruster, a subsonic flow is successfully accelerated to a supersonic one by converting ion thermal energy to flow energy. However, flow velocity is found to decrease suddenly in the diverging region of the Laval nozzle. By using a magnetic Laval nozzle with a gentle gradient in the diverging region, flow velocity increases smoothly and a supersonic flow is obtained in the uniform magnetic field region.

Nomenclature

I_d	=	discharge current	A	=	effective cross section of plasma
J_r	=	radial component of current density	μ	=	magnetic moment
B_z	=	axial component of magnetic field	r_p	=	plasma radius
B_θ	=	azimuthal component of magnetic field	ρ_e	=	Larmour radius of electron
U_z	=	axial component of plasma flow velocity	ρ_i	=	Larmour radius of ion
U_θ	=	azimuthal component of plasma flow velocity			
U	=	total plasma flow velocity			
M_i	=	ion acoustic Mach number			
γ_i	=	specific heat ratio of ions			
γ_e	=	specific heat ratio of electrons			
m_i	=	mass of ion			
T_i	=	ion temperature			
T_e	=	electron temperature			
n_e	=	number density of electrons			
n_i	=	number density of ions			
W_{thermal}	=	plasma thermal energy			
W_{flow}	=	plasma flow energy			

* Professor, Department of Electrical Engineering, inutake@ecei.tohoku.ac.jp.

† Associate Professor, Department of Electrical Engineering, akira@ecei.tohoku.ac.jp.

‡ Researcher, Department of Electrical Engineering, hattori@ecei.tohoku.ac.jp..

§ Researcher, Department of Electrical Engineering, tobari@ecei.tohoku.ac.jp.

** Graduate student, Department of Electrical Engineering, harata@ecei.tohoku.ac.jp.

†† Graduate student, Department of Electrical Engineering, komagome@ecei.tohoku.ac.jp

I. Introduction

ELECTRIC propulsion (EP) is one of the most promising space propulsions with a high specific impulse I_{sp} which is defined by a ratio of a thrust to a propellant weight flow rate, representing a propellant exhaust velocity divided by the gravity acceleration. This system utilizes the electric energy to ionize a propellant gas that is accelerated by electro-thermal, electrostatic or electromagnetic effects. Since ionized propellant is exhausted downstream of the thruster with a velocity much higher than that in a chemical rocket, EP system enables a long-term space mission with less consumption of the propellant. Recently, they are utilized not only for an attitude or position control for various satellites but also for a main engine in deep-space explorations. In an asteroid-sample-return project of ISAS (JAXA), Japan launched a spacecraft "HAYABUSA" in May, 2003.^{1,2} The main engine consists of 4 ion engines which utilize an ECR(electron cyclotron resonance) produced plasma instead of a conventional filament or hollow cathode discharge plasma. Various types of advanced space propulsion devices have been proposed and under development in order to be utilized not only in a main engine for a small spacecraft but for a large-sized, long-term space missions, such as a manned Mars exploration and an earth-impact-asteroid de-orbiting.³

For a manned interplanetary space thruster, both a higher specific impulse and a larger thrust are required. Until the realization of a fusion-plasma thruster, a magnetoplasmadynamic thruster (MPDT) driven by a fission reactor is one of the promising candidates for a manned Mars spacecraft. An MPDT plasma is accelerated axially by self-induced $j \times B$ force.³ A pulsed MPDT of ISAS (JAXA), Japan driven by a solar cell was tested on board a space laboratory SFU launched by the H-II rocket of NASDA (JAXA), Japan in March, 1995 and retrieved by the space shuttle Endeavor of NASA, USA in January, 1996. The MPDT was successfully operated for 40,000 shots with I_{sp} of 1,100 sec.⁴

An MPDT has high-thrust density, which is proportional to the square of the discharge current, and so thrust efficiency is improved in a higher current operation. Characteristics of an expanding plasma from an applied-field MPDT were investigated experimentally^{5,6} and thrust performance of an MPDT was found to be improved by applying an external magnetic nozzle instead of a solid nozzle.⁷⁻⁹ An applied-field MPDT operation will help reduce erosion of electrodes and diffuse current attachment, which are crucial problems for a steady-state and high-current operation of an MPDT. Plasma acceleration mechanism, however, becomes very complicated due to the addition of $j_r \times B_z$ rotational, $j_\theta \times B_r$ Hall and magnetic-nozzle accelerations.¹⁰ It is important to clarify effect of the magnetic field and to obtain an optimum magnetic nozzle configuration in the vicinity of an MPDT outlet for the improvement of thrust efficiency.

In order to investigate effects of the external magnetic field on MPDT characteristics, we have studied a plasma flow produced by an MPDT in detail by use of a spectrometer and Mach probes in the HITOP device, Tohoku University.¹¹⁻¹³ In our previous experimental works, it was found that an ion Mach number M_i of an MPDT plasma with a uniform magnetic field was limited below unity even in a high current operation. When the discharge current increases up to 10kA, a plasma flow velocity increased almost linearly with the current. Whereas, an ion temperature suddenly increased when the discharge current becomes more than 8kA, resulting in the limitation of M_i less than unity in the vicinity of the MPDT. In such a high current region, an input electric energy was converted to a thermal energy rather than a flow energy, leading to undesirable ion heating. Several attempts such as measurements of spatial profiles of induced magnetic fields by a magnetic probe array have been performed to clarify mechanisms of the ion heating and the Mach number limitation.^{14,15}

It is very important to develop an optimum magnetic nozzle configuration in the vicinity of an MPDT for converting a high ion thermal energy to an axial flow energy and for improving its thrust efficiency. In order to verify the magnetic nozzle effect on the MPDT plasma, we attached a small-sized magnetic coil with a shorter characteristic length. A Laval-type magnetic nozzle configuration is formed in the outlet region of the MPDT and its effects on the spatial variation of plasma parameters are measured by use of a spectrometer and Mach probes. It is expected that the subsonic flow near the MPDT is converted to a supersonic flow through the magnetic Laval nozzle as in a conventional compressible gas flow.

In this paper we present characteristics of a plasma flow produced by an MPDT with additional magnetic nozzle configurations. Spatial variations of plasma parameters are discussed in comparison with one-dimensional isentropic fluid equations in a compressible gas.

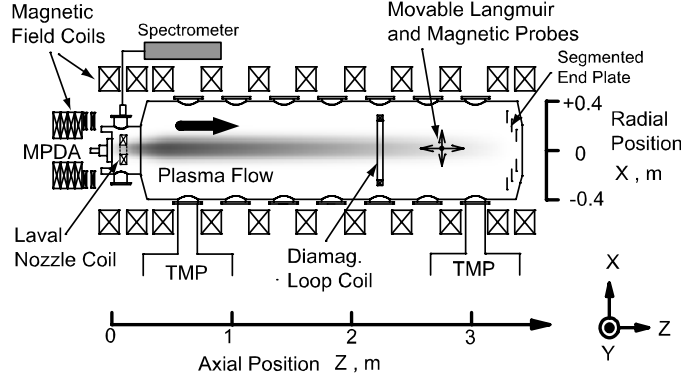


Figure 1. Schematic view of the HITOP device.

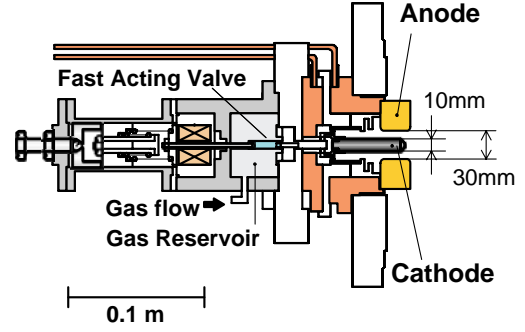


Figure 2. A side view of the MPD thruster.

II. Experimental apparatus

A. HITOP device

Experiments are performed in the HITOP (High density TOhoku Plasma) device of Tohoku university⁵⁻⁷. The HITOP device consists of a large cylindrical vacuum chamber (diameter $D = 0.8$ m, length $L = 3.3$ m) and 11 main and 6 auxiliary external magnetic coils, which can generate a uniform magnetic field up to 1kG, as shown in Fig.1. Although various types of magnetic field configurations can be formed by adjusting these coil currents, a uniform magnetic field B_0 of 0.087T is applied by these coils in the present experiments. A high-power, quasi-steady MPDT is installed at one end of the HITOP device. A schematic view of the MPDT is shown in Fig. 2. It has a coaxial structure with a center tungsten rod cathode (10 mm in outer diameter) and an annular molybdenum anode (30 mm in inner diameter). A fast acting gas valve can inject helium gas quasi-steadily for 3ms. After the gas valve is open, discharge current I_d up to 10kA is supplied by a pulse-forming network (PFN) system with a quasi-steady duration of 1ms. The current can be increased to 15kA with a shorter quasi-steady duration of 0.4ms. The current I_d can be controlled by varying the charging voltage of the PFN power supply. The coordinate direction of X, Y and Z-axes are shown in Fig.1 and 2. The position $Z=0$ is located at the cathode tip of the MPDT.

B. Diagnostics

Spectroscopic diagnostics are used to measure an ion temperature T_i , axial and azimuthal (rotational) flow velocities U_z , U_θ in the outlet region of the MPDT. The ion temperature and flow velocities are obtained from Doppler broadening and spectral shift of line spectra. Emission from the plasma is collected by a quartz lens and is transferred to a spectrometer by a single fiber cable. A line spectrum is detected with an image intensifier tube coupled with a CCD camera set at the exit plane of a Czerny-Turner spectrometer with a focal length of 1 m and a grating 2400 grooves/mm. In case of helium gas, HeII line spectra ($\lambda = 468.58$ nm) are obtained in every 0.1msec time interval during a shot with the spectral resolution of 0.02nm and time evolutions of T_i , U_z and U_θ are obtained.

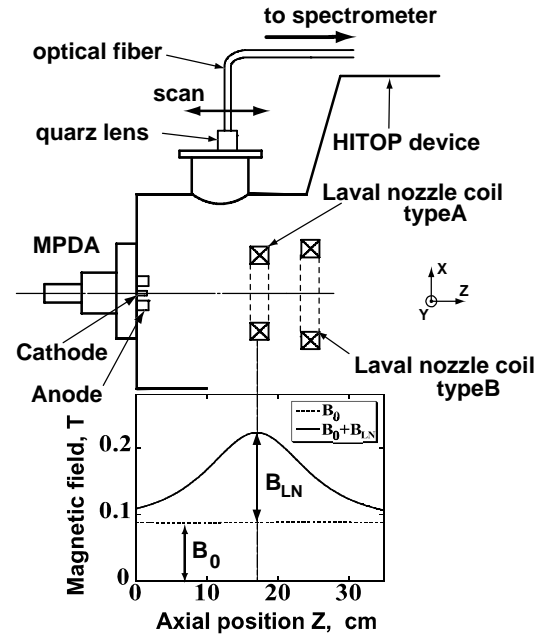


Figure 3. Layout of alternatively used two types of Laval-nozzle coils. Axial profiles of the magnetic field near the MPDT are shown in case of type-A coil (B_{LN}) in addition to a uniform field (B_0).

Electron temperature and density profiles are measured by a movable triple probe and a fast-voltage-scanning Langmuir probe. An ion Mach number M_i is also measured by a movable Mach probe¹⁶ and an array of 13-channel Mach probes set at 1.7m downstream of the MPDT. Time-varying magnetic fields in the plasma flow are measured directly by a movable magnetic probe array.

C. Laval nozzle coils

In order to closely investigate a Laval nozzle effect on a thermal energy conversion to a flow energy, a short magnetic Laval nozzle configuration is formed near the MPDT outlet.

Small-sized additional coils, type-A and B are installed in the vicinity of the MPDT. Fig.3 shows an arrangement of the coils and axial profiles of the resultant magnetic field. Two types of the coils (type-A and type-B with the inner diameters of 20cm and 24cm, respectively) are used. As the location of the coils and coil currents can be changed, we can investigate effects of the nozzle shape on the exhaust plasma parameters in order to optimize the magnetic Laval nozzle configuration.

III. Experimental results

A. Effect of the magnetic Laval nozzle

Firstly, a magnetic Laval nozzle configuration is formed by using only the type-A coil. We measured axial variations of T_i and U in both upstream and downstream regions of the magnetic throat in order to clarify mechanism of the magnetic Laval nozzle. Figure 4 shows axial profiles of a magnetic field, an effective cross section of the plasma A , T_i , U_z and M_i . The effective cross section is estimated from a radial profile of the light emission intensity. The profile is almost Gaussian and a plasma radius is derived from the e-folding length of the profile.

Total flow velocity U of the MPDT has two dominant components, that is, axial velocity U_z and azimuthal velocity U_θ . These velocities are measured simultaneously by the spectrometer. The velocity U is derived as

$$U = \sqrt{U_z^2 + U_\theta^2} \quad (1)$$

An ion Mach number of the plasma M_i is derived by using T_i and U and related to the ratio of a plasma flow energy to a thermal energy,

$$M_i = \frac{U}{C_s} = \frac{U}{\sqrt{(\gamma_i T_i + \gamma_e T_e)/m_i}} \\ = \sqrt{\frac{\frac{1}{2}(n_e + n_i)m_i U^2}{\gamma_i n_i T_i + \gamma_e n_e T_e}} = \sqrt{\frac{W_{flow}}{W_{thermal}}} \quad (2)$$

Here γ_i and γ_e are the specific heat ratio of ions and electrons, respectively, and m_i is the mass of a helium ion. We assumed $\gamma_i=5/3$, $\gamma_e=1$ and $T_e=5\text{eV}$ in the calculation of M_i in Fig.4.

It is clearly shown in Fig.4 that the ion temperature decreases and the flow velocity increases when the plasma passes through the Laval nozzle. M_i also increases from a subsonic value ($M_i < 1$) to a supersonic one ($M_i > 1$). M_i

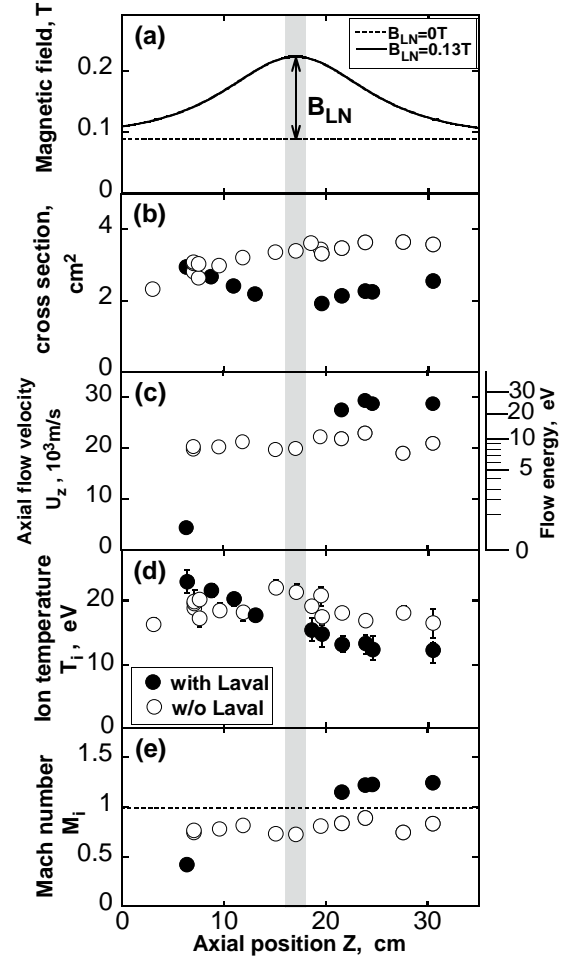


Figure 4. Axial profiles of flow characteristics with (solid circles) and without (open circles) the Laval nozzle. A subsonic flow is converted into a supersonic one passing through the magnetic Laval nozzle. $I_d=7.2\text{kA}$.

attains unity at the nozzle throat, which is the same behavior as in a compressible gas. In the upstream region of the nozzle, these variations of the flow parameters are reversed: that is, T_i becomes higher and U_z and M_i become lower in the case with the nozzle. This shows that the subsonic flow upstream of the nozzle perceives the existence of the nozzle and self-adjusts so as to satisfy the sonic condition at the nozzle throat.

Figure 5 shows flow characteristics measured at $Z=30.5\text{cm}$ in the downstream region of the Laval nozzle as a function of I_d . As I_d increases, U_z and T_i increases in proportion to the current but T_i abruptly increases above $I_d=8\text{kA}$ in the case without the Laval nozzle. By applying the Laval nozzle in the outlet region of the MPDT, the increase of T_i is suppressed and U_z increases additionally and as a consequence, M_i keeps the value above unity in the downstream region.

It is also confirmed that the total energy, sum of the flow energy and the thermal energy, in the cases with and without the Laval nozzle agrees well with each other within an experimental error. This indicates that thermal energy successfully is converted to the flow energy by the magnetic Laval nozzle.

B. Behavior as a plasma fluid

When a plasma is collisionless and highly magnetized, ions and electrons gyrate in the Larmour motion many times between collisions. The kinetic energy of the charged particles parallel and perpendicular to the magnetic field changes according to the magnetic field strength so as to keep the magnetic moment, $\mu=(1/2)mv_{\perp}^2/B$, constant. As a consequence, there should not occur any change in the plasma flow velocity upstream and downstream of the magnetic Laval nozzle, since there is no difference in the magnetic field strength.

Under the present experimental conditions, however, the exhausted plasma density is more than 10^{20} m^{-3} and the magnetic field strength is relatively weak around 0.1T . The Hall parameters of electrons and ions, $\omega_{ce}\tau_{ee}$ and $\omega_{ci}\tau_{ii}$, are calculated along the Z -axis as shown in Fig.6. Ratios of the Larmour radius to the plasma radius r_p derived by spectroscopy for electrons and ions, ρ_e/r_p and ρ_i/r_p , are also shown in the figure. Since the Hall parameter of ions is less than unity, the ions do not magnetized in the region of the Laval nozzle. Ions collide with each other so frequently that they behave as an ion fluid. Whereas, the electrons are magnetized in the nozzle region and the electron Larmour radius is much less than the plasma radius. Then the motion of electrons in the plasma flow is constrained by a magnetic field line.

Although the ions behave as a fluid, its boundary in radial direction is affected by the behavior of the electrons, which are constrained by the magnetic field, due to the ambipolar radial electric field. Therefore, ions act as a continuum medium bounded by the magnetic field configuration. This mechanism plays an important roll for making the magnetic Laval nozzle effective.

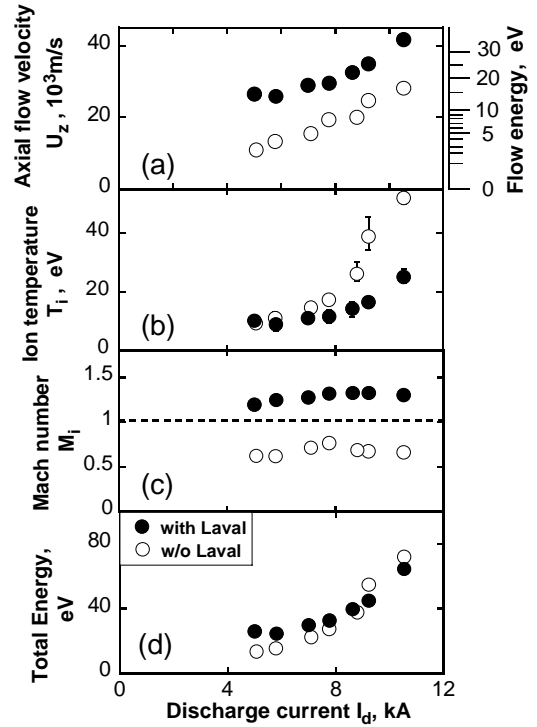


Figure 5. Flow characteristics with (solid circles) and without (open circles) the Laval nozzle as a function of discharge current of the MPDT measured in the downstream region of the Laval nozzle ($Z=30.5\text{cm}$).

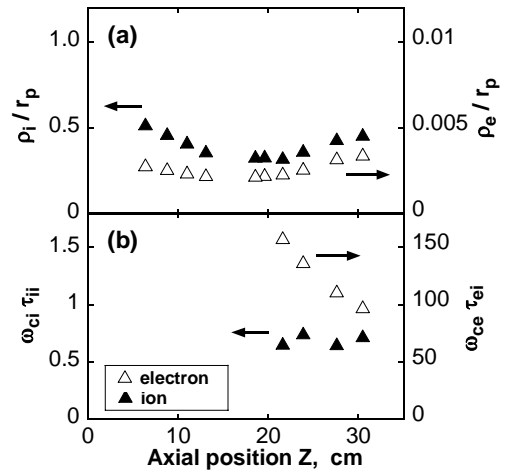


Figure 6. Axial profiles of (a) ratios of a Larmour radius to a plasma radius, ρ_e/r_p and ρ_i/r_p , and (b) Hall parameters, $\omega_{ce}\tau_{ee}$ and $\omega_{ci}\tau_{ii}$, for electrons and ions.

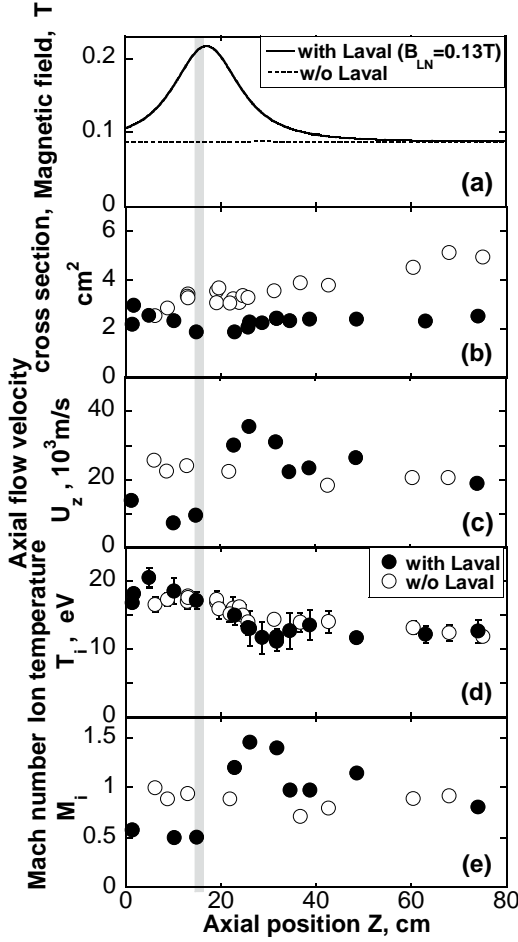


Figure 7. Axial profiles of (a) B_z , (b) plasma cross section measured by spectroscopy A , (c) U_z , (d) T_i , and (e) M_i , with and without the type-A magnetic Laval nozzle coil. $I_d=7.2\text{kA}$, $B_0=0.087\text{T}$.

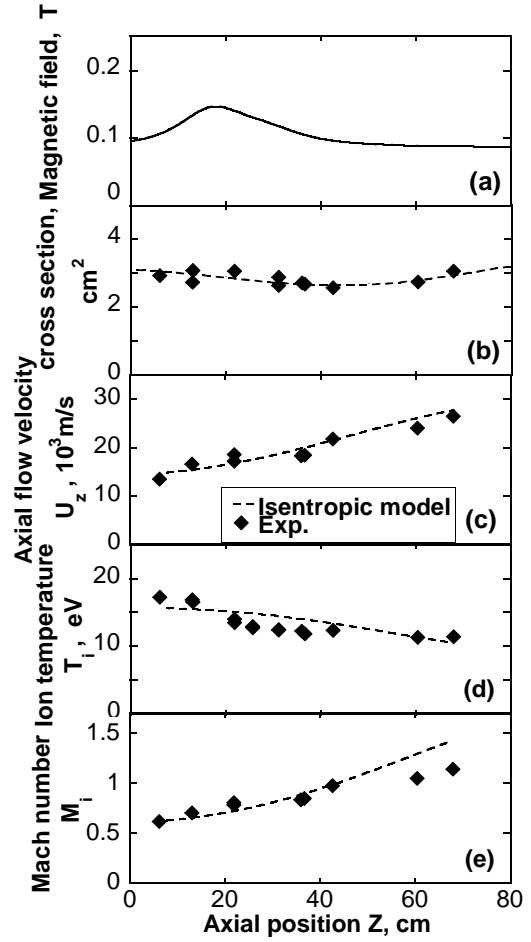


Figure 8. Same as in Fig.7 using the type-A and B Laval nozzle coils. Dotted lines corresponds to predicted value by 1-D isentropic flow model.

In terms of a one-dimensional isentropic flow model in a compressible gas, the Mach number is related to variation of the cross-sectional area A of the flow channel,

$$\frac{dM}{M} = \frac{2 + (\gamma - 1)M^2}{2(M^2 - 1)} \frac{dA}{A} \quad (3)$$

Also, the flow velocity U , the temperature T and the mass density ρ vary as follows,

$$\frac{dU}{U} = \frac{1}{(M^2 - 1)} \frac{dA}{A} \quad (4)$$

$$\frac{dT}{T} = -\frac{(\gamma - 1)M^2}{(M^2 - 1)} \frac{dA}{A} \quad (5)$$

$$\frac{d\rho}{\rho} = -\frac{M^2}{(M^2 - 1)} \frac{dA}{A} \quad (6)$$

Assuming that the flow-channel area A varies according to the magnetic flux conservation in vacuum $B_0 A = \text{const.}$, the axial profiles of U , T and M are calculated from the above Hugoniot equations. The measured variations of U , T_i and M_i through the Laval nozzle are compared with those predicted by the 1-D isentropic flow model and are in agreement with each other. Quantitatively, M_i measured downstream of the nozzle throat is lower than the predicted one. This would be due to an under-expansion expected from the observation that the cross section of the

plasma flow downstream of the throat does not coincide with that of the vacuum magnetic channel. In addition, recent experiments show that effects of the strong diamagnetism and the high dynamic pressure of the high density MPDT plasma deform the external magnetic field. These deformation effects of the nozzle configuration should be taken into consideration for a better prediction.

C. Shaping of the nozzle

The magnetic Laval nozzle can improve the exhaust plasma parameters as mentioned above. It is observed, however, that the flow velocity begins to decrease abruptly at some point in the diverging region of the Laval nozzle as shown in Fig.6. This phenomenon is presumably related to a shockwave in the diverging region of the nozzle as was observed in the previous researches.^{5,6}

In order to avoid this phenomenon, a magnetic field with a more gentle gradient in the diverging region is formed by using type-A and B nozzle coils. When this nozzle is used, the abrupt decrease of M_i in the downstream region tends to disappear. The flow velocity increases smoothly and M_i gradually increases more than unity, and then a supersonic flow is obtained in the uniform magnetic field region as shown in Fig.7. As shown also in the figure, spatial variations of plasma parameters are similar to those predicted by the 1-D isentropic flow model, as far as the measured cross sectional area is used instead of the area predicted by a vacuum flux tube.

This experiment indicates that precise control of the Laval-type magnetic nozzle is necessary in order to improve the thrust performance. It is also noted that the magnetic nozzle ratio should be optimized in both the converging and the diverging region by taking into account effects of a high plasma pressure and a high dynamic pressure of a fast flow.

IV. Conclusion

A magnetoplasma dynamic thruster (MPDT) with an externally-applied magnetic Laval nozzle is investigated to improve the plasma flow exhausted from an MPDT. Small-sized coils with a shorter characteristic length are attached near the outlet of an MPDT to form a Laval-type magnetic nozzle. A plasma flow velocity increases and an ion temperature decreases as the plasma passes through the magnetic Laval nozzle. An ion Mach number increases from a value below unity to above unity. Increment of the plasma exhaust velocity is related to the increase in thrust and specific impulse and results in the improvement of the MPDT performance. A subsonic flow near the outlet is successfully accelerated to a supersonic flow by converting ion thermal energy to flow energy as is in a conventional compressible gas flow. These results are consistent with the prediction from the 1-D isentropic flow model.

However, flow velocity is found to decrease abruptly after attaining a peak of the Mach number in the downstream region of the nozzle throat. By using a magnetic Laval nozzle with a gentle gradient in the diverging region, the flow velocity increases smoothly, leading to a supersonic flow.

Acknowledgments

This work was supported in part by Grant-in-Aid for Scientific Researches from Japan Society for the Promotion of Science.

References

- ¹Kuninaka H., et al., "Flight Report During Two Years on HAYABUSA Explorer Propelled by Microwave Discharge Ion Engines," *Proceedings of 41st Joint Propulsion Conference and Exhibit*, AIAA-2005-3673, 2005.
- ²Funaki I., Kuninaka H., and Toki K., "Plasma Characterization of a 10-cm Diameter Microwave Discharge Ion Thruster," *J. of Propulsion and Power*, Vol.20, No.4, 2004, pp.718-727.
- ³Jahn R.G., *Physics of Electric Propulsion*, McGRAW-HILL, 1968.
- ⁴Toki K., Shimizu Y., and Kuriki K., "On-Orbit Demonstration of a Pulsed Self-Field Magnetoplasma dynamic Thruster System," *J. of Propulsion and Power*, Vol.16, No.5, 2000, pp.880-886.
- ⁵Kuriki K. and Okada O., "Experimental Study of a Plasma flow in a Magnetic Nozzle," *Phys. Fluids*, Vol.13, No.9, 1970, pp.2262-2269.
- ⁶Kuriki K. and Inutake M., "Super-Alfvénic Flow and Collision-free Shock-wave in a Plasma Wind-tunnel," *Phys. Fluids*, Vol.17, No.1, 1974, pp.92-99.
- ⁷Sasoh A., and Arakawa Y., "Electromagnetic effects in an applied-field magnetoplasma dynamic thruster," *J. of Propulsion and Power*, Vol.8, No.1, 1992, pp.98-102.
- ⁸Tahara H., Kagaya Y., and Yoshikawa T., "Performance and Acceleration Process of Quasisteady Magnetoplasma dynamic Arcjets with Applied Magnetic Fields," *J. of Propulsion and Power*, Vol.13, No.5, 1997, pp.651-658.

⁹Krülle G., Auweter-Kurtz M., and Sasoh A., "Technology and Application Aspects of Applied Field Magnetoplasma-dynamic Propulsion," *J. of Propulsion and Power*, Vol. 14, No. 5, 1998, pp.754-763.

¹⁰Sasoh A., and Arakawa Y., "Thrust Formula for Applied-Field Magnetoplasma-dynamic Thrusters Derived from Energy Conservation Equation," *J. of Propulsion and Power*, Vol.11, No.2, 1995, pp.351-356.

¹¹Ando A., et al., "Spectroscopic Studies of a High Mach-Number Rotating Plasma Flow," *Journal of Plasma Fusion Research, SERIES*, Vol.4, 2001, pp.373-378.

¹²Inutake M., et al., "Characteristics of a Supersonic Plasma Flow in a Magnetic Nozzle," *Journal of Plasma Fusion Research*, Vol.78, 2002, pp.1352-1360. URL:http://jasosx.ils.uec.ac.jp/JSPF/JSPF_TEXT/jspf2002/jspf2002_12/jspf2002_12-1352.pdf [cited 3 October 2005].

¹³Inutake M., et al., "Magnetic-Nozzle Acceleration and Ion Heating of a Supersonic Plasma Flow," *Transactions of Fusion Technology*, Vol.43, No.1T, FUSTE8, 2002, pp.118-124.

¹⁴Tobari, H., Inutake, M., Ando, A. and Hattori, K., "Spatial Distribution of Lorentz Forces in an Applied-Field Magneto-Plasma-Dynamic Arcjet Plasma," *Journal of Plasma Fusion Research*, Vol.80, 2004, pp.651-652. URL: http://jasosx.ils.uec.ac.jp/JSPF/JSPF_TEXT/jspf2004/jspf2004_08/jspf2004_08-651.pdf [cited 3 October 2005].

¹⁵Tobari, H., Ando, A., Inutake, M., and Hattori, K., "Direct Measurement of Lorentz Forces in an Applied-Field MPD Thruster," *Proceedings of the 29th International Electric Propulsion Conference, IEPC-2005-65*, 2005.

¹⁶Ando, A. et al., "Evaluation of Para-Perp Type Mach Probe by Using a Fast Flowing Plasma" *Journal of Plasma Fusion Research*, Vol. 81, 2005, pp.451-457. URL:http://www.jspf.or.jp/Journal/PDF_JSPF/jspf2005_06/jspf2005_06-451.pdf [cited 3 October 2005].